IEEE Access
Multidisciplinary | Rapid Review | Open Access Journal

Date of publication xxxx 00, 0000, date of current version xxxx 00, 0000.

Digital Object Identifier 10.1109/ACCESS.2017.DOI

Statistical Approximation of Plantar Temperature Distribution on Diabetic Subjects based on Beta Mixture Model

D. HERNANDEZ-CONTRERAS[1], H. PEREGRINA-BARRETO[1], J. RANGEL-MAGDALENO[1], AND F. ORIHUELA-ESPINA[1]

[1]Instituto Nacional de Astrofisica, Optica y Electronica (INAOE), Luis Enrique Erro No. 1, 72840 Puebla, Mexico

Corresponding author: Jose Rangel-Magdaleno (e-mail: jrangel@inaoep.mx).

ABSTRACT A change in plantar temperature distribution can be an indicator of tissue damage, inflammation or peripheral vascular abnormalities associated with diabetic foot. Despite the efforts to detect these abnormalities through infrared thermography, there are still several problems to be addressed, especially to detect abnormalities on each foot separately. In this work, a characterization of the plantar temperature distribution based on a probabilistic approach is proposed. The objective is to detect temperature variations on each foot eluding contralateral comparison. A beta mixture model with 4 components approximates the plantar temperature distributions of diabetic and non-diabetic subjects. Each component represents an area of the plantar region: toes, metatarsal heads, arch and heel. The approximation was applied to 60 temperature distributions of non-diabetic subjects and 220 of diabetic subjects. The results suggest that it is possible to characterize distribution in terms of the mean of its beta components.

INDEX TERMS Beta mixture model, diabetes mellitus, diabetic foot, infrared thermography.

I. INTRODUCTION

Diabetes mellitus (DM) is a chronic and complex disease that requires early and continuous medical care to prevent complications [1]. In 2015, it was estimated that diabetes was the direct cause of 1.6 million deaths and according to projections of the World Health Organization (WHO), diabetes will be the seventh cause of mortality in 2030 [2]. The global prevalence of DM in adults (over 18 years of age) has increased from 4.7% in 1980 to 8.5% in 2014, representing a growing health problem worldwide [2]. The diabetic foot is a common complication experienced by diabetic patients, and it can be defined as an infection, ulceration and/or destruction of deep tissues associated with neurological abnormalities and various degree of peripheral vascular disease (PVD) in the lower limb [3]. Diabetic foot ulcer, mainly related to peripheral neuropathy and peripheral arterial disease (PAD), is the most common presign of the lower limb amputation.

People with neuropathy often have a loss of feeling, foot deformation and limited joint mobility producing an abnormal biomechanical foot load [4]. A study conducted by [5] confirmed that elevated plantar pressures are strongly predictive of subsequent ulceration, especially in the presence of neuropathy. The excessive pressures in the plantar region can cause tissue damage or inflammation, leading to an increase in skin temperature. The skin temperature can also be affected by changes in the blood flow [6]. PAD rarely leads to foot ulceration. However, it is an important risk factor for wound healing because, once ulceration develops, it prolongs the healing time, thereby increasing the risk of amputation [7].

Infrared thermography (IRT) is a widely used technique for temperature monitoring, and it has been used in several medical applications [8]–[11]. IRT is a non-contact, non-intrusive and non-invasive technique, with an advantage of no direct alteration in the surface temperature and its ability to display real time surface temperature distribution [12]. There is a wide investigation about automatic identification of complications derived from diabetic foot using IRT [13]–[19]. Nagase et al. [15] proposed a classification system with 20 categories of thermal patterns in the plantar region based on the angiosome concept. Mori et al. [16] proposed a new classification system for plantar thermographic patterns by a segmentation algorithm based on a mode-seeking method. In [19], it is reported a methodology to obtain quantitative information about the temperature difference in the plantar area to detect ulceration risk. They proposed two estimators:

This article has been accepted for publication in a future issue of this journal, but has not been fully edited. Content may change prior to final publication. Citation information: DOI 10.1109/ACCESS.2019.2902502, IEEE Access

an estimated difference (ETD) to determine if exist any abnormal temperature difference, and a Hot Spot Estimator (HSE) to detect small abnormal areas with high temperature. The results were that the HSE detected abnormal regions in initial phase that the ETD was incapable to detect. More recently, Hernandez-Contreras et al. [13] presented a classification system to identify temperature patterns associated to healthy and diabetic subjects. They obtain a classification rate of 94.33 %. For further details about studies related to temperature analysis with IRT, the reader is invited to read these reviews [20], [21].

Asymmetric temperature analysis is the most common approach due to its simplicity. It consists in comparing the temperature of one foot with its contralateral. By this comparison and by defining a threshold, it is possible to detect risk areas. Liu et al. [17] presented a methodology to evaluate the effectiveness of IRT to detect diabetic foot complications through asymmetric analysis. The detection of foot complications was calculated by the subtraction of temperature values, corresponding to pixels in the right and left foot and the risk spots were identified using a hard threshold of 2.2 °C in each pixel. With this threshold, they were able to identify 35 of 37 diabetic patients. Kaabouch et al. [14] presented a technique that allows reliable comparison even if the shapes and sizes of the two foot projections are different. Although this method is the most used, it has important limitations. For example, if the patient has similar complications in both feet, asymmetrical analysis cannot detect most risk areas; if the patient has a partial or total amputation in one foot, there will not be an area with which to compare. For these reasons, it is important to develop techniques to complement this type of analysis to overcome these limitations.

Based on this information, we hypothesized that a characterization of the distribution can be useful to detect variations in the plantar temperature distribution without the need of a contralateral comparison, and in this way to be able to analyze each foot separately. To prove this hypothesis, a beta mixture model (BMM) is used to model the plantar temperature distributions of diabetic and non-diabetic subjects. The distributions are approximated by 4 components, each representing an area of the plantar region: toes, metatarsal heads, arch and heel. The four areas were chosen based on the high pressure areas and the symmetric butterfly pattern reported by Chan et al. [22]. Finite mixture models have been widely used in several applications of classification and clustering for several years [23]. In contrast with other distributions such as Gaussian, the Beta distribution has the advantage of a defined interval in addition to being able to take a variety of symmetric and asymmetric forms, since it can be skewed to the right, skewed to the left or be symmetric [24]. The BMM was applied to 280 plantar distributions (60 of non-diabetic subjects and 220 of diabetic subjects). The performance of the of the BMM approach was compared with other models: Gaussian mixture model and Gamma mixture model.

This paper is organized as follows. In Section II, details of the methodology, as well as an introduction to some concepts relevant for the modeling are presented. In Sections III and IV, the experimental results and discussion of the results are described. Finally, the conclusion of this work is presented in Section V.

II. METHODOLOGY

The proposed methodology starts with the acquisition and segmentation of the plantar region. After that, the foot position is corrected in order to obtain the temperature distribution. A histogram is obtained based on this distribution. Finally, the observations are modeled by a BMM with 4 components.

A. THERMOGRAM ACQUISITION

The study involved 141 volunteers split into 2 groups: 30 non-diabetic subject forming the control group, and 111 subjects diagnosed with DM type 2 who form the DM group. The subjects were recruited from the Hospital General del Norte, Hospital General del Sur and from the Instituto Nacional de Astrofisica, Optica y Electronica. All of these places are located in Puebla city, Mexico. The subjects were informed about the test and voluntarily agreed to participate. In the DM group, all feet with infection, ulcer or partial amputation were excluded from the tests, and only the remaining foot of the subject was used. Two feet were excluded based on this criterion.

For thermogram acquisition, an infrared camera FLIR E60 with a thermogram resolution of 320×240 pixels and a thermal sensitivity less than 0.05 °C was used. The recommendations of the International Academy of Clinical Thermology were followed [25]. Thermograms were captured in a room at controlled temperature of 20 ± 1 °C. The proper preparation of the subjects consists of asking them to remove their shoes and socks and clean their feet with a damp towel. After that, the subjects were invited to maintain a supine position for 15 minutes. An obstructive IR device was placed to isolate the plantar temperature from the rest of the body, and finally, the thermogram was captured. During the acquisition of thermograms, patients were in complete rest and sometimes they were unable to keep their feet in vertical position. Although this inclination can affect subsequent analysis, if any device is placed to maintain this position, the blood pressure can be affected and therefore, the temperature will also be affected. Hence, we corrected the foot posture digitally (see section II-C).

For better visualization, the thermograms in this study are presented with a color palette and a scale ranging from 20 to 36 °C. However, a raw temperature file was used for the tests. This file is generated by the infrared camera, and it has the temperature of each pixel in the image with a precision of three decimals.

This article has been accepted for publication in a future issue of this journal, but has not been fully edited. Content may change prior to final publication. Citation information: DOI 10.1109/ACCESS.2019.2902502, IEEE Access

B. SEGMENTATION OF THE PLANTAR REGION

To isolate the plantar region in the thermogram, a binary mask obtained by a thresholding method is used. The threshold is automatically optimized from the histogram, as detailed in [13]. With a bimodal distribution of the histogram representing the plantar region and the background of the thermogram, the threshold is obtained based on the minimum value between the two maximums [13]. Once the plantar region is isolated, the thermograms are split into two images, one for each foot. These single foot images are used in the subsequent analysis.

C. FEET POSITION CORRECTION

The foot posture was corrected by the process described in the previous work [26]. In brief, the correction was based on three reference points: the tip of the innermost toe (A), the center of the calcaneal base (B), and the third one (C) is placed in the same vertical position as point B (Fig. 1). After several tests, it was determined that an angle of 85 ° on the inside of the foot, between the BA and BC axes, indicated a vertical feet position.

FIGURE 1. Reference points to correct feet posture.

D. TEMPERATURE DISTRIBUTION

With the position of the foot corrected, the temperature profile distribution is obtained calculating the average temperature for each column of the plantar thermogram, as shown in Fig. 2. Values equal to zero are excluded from the average temperature because these are not part of the plantar region.

E. HISTOGRAM CREATION BASED ON PLANTAR TEMPERATURE DISTRIBUTION

The histograms of the temperature distributions were offset corrected, closed by extrapolation and normalized. The offset of each distribution is removed by subtracting the minimum temperature value, which is at the beginning or end of the

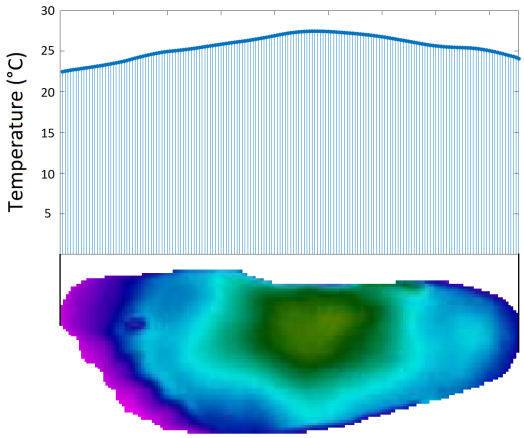

FIGURE 2. An example of the plantar temperature distribution from the control group, and its associated marginalization of temperatures across the y-axis..

temperature distribution (Fig. 3b). Then the other side is extrapolated to the intersection with zero by a Lagrange polynomial (Fig. 3c). The histogram is formed where the frequency is represented by the average temperature of each column of the thermogram. An accuracy of three decimals is chosen to detect changes in temperature from one pixel to another (Fig. 3d). The X-axis of the histogram is bounded to the same interval of the beta distribution [0,1] (see Section II-F).

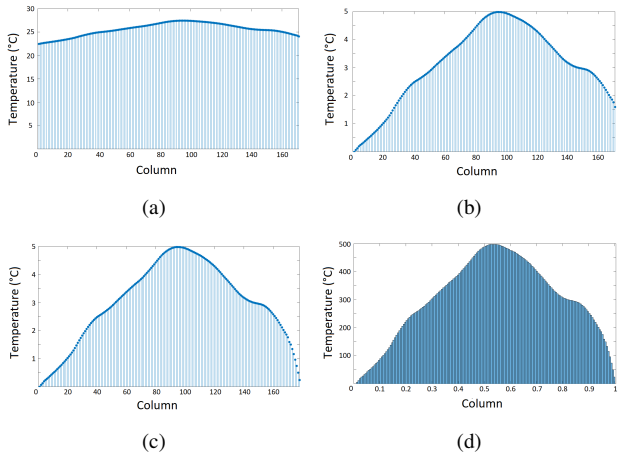

FIGURE 3. Processing of the histogram of the temperature distribution. (a) Raw temperature distribution; (b) offset correction; (c) extrapolation; and (d) normalization.

F. BETA MIXTURE MODEL (BMM)

Once the final processed histogram is obtained, an approximation is estimated from a Beta mixture model. The beta distribution is a continuous probability distribution with two real positive parameters (α and β) [27], [28] and defined on the interval [0,1].

This article has been accepted for publication in a future issue of this journal, but has not been fully edited. Content may change prior to final publication. Citation information: DOI 10.1109/ACCESS.2019.2902502, IEEE Access

$$Beta(x \mid \alpha, \beta) = \frac{\Gamma(\alpha+\beta)}{\Gamma(\alpha)\Gamma(\beta)} x^{\alpha-1}(1-x)^{\beta-1} \quad (1)$$

where $\Gamma(\cdot)$ is the gamma function. Given a d-dimensional data vector $X = (x_1, x_2, ..., x_d)$, a density of a BMM is defined by:

$$f(X \mid \vartheta) = \sum_{c=1}^{C} \pi_c Beta(X \mid \alpha_c, \beta_c) \quad (2)$$

where C is the number of components of the mixture model, π_c is the c_{th} mixing proportion such that $\pi_c > 0$ and $\sum_{c=1}^{C} \pi_c = 1$, and $\vartheta = (\pi_1, ..., \pi_c, \alpha_c, ..., \alpha_c, \beta_1, ..., \beta_c)$ is the vector of parameters. The parameter vector ϑ for maximum likelihood estimation was done through the Expectation-Maximization (EM) algorithm.

1) Maximum Likelihood Estimation (MLE)

Given a set of data $X = \{x_1, x_2, ..., x_N\}$, where x is a scalar value, the MLE approach can be used to find the parameters that fit the observed data. The aim is to find the parameter vector ϑ that maximizes the log-likelihood function: [23], [29], [30].

$$L(\vartheta \mid X) = log \prod_{n}^{N} \prod_{c}^{C} [\pi_n Beta(x_n \mid a_c, b_c)]^{z_{nc}} \quad (3)$$

$$L(\vartheta \mid X) = \sum_{n}^{N} \sum_{c}^{C} z_{nc}[log\pi_c + logBeta(x_n \mid a_c, b_c)] \quad (4)$$

where z_{nc} indicates if x_n belongs or does not belong to the component c.

2) Expectation-Maximization algorithm

The EM algorithm is an iterative method with two steps, expectation (E) and maximization (M), for ML parameter estimation with incomplete data. In the E-step, the expected values (z_{nc}) are calculated as the posterior probability of x_n, being generated from the c component (5) [27].

$$z_{nc} = \frac{\pi_c Beta(x_n \mid \alpha_c, \beta_c)}{\sum_{k=1}^{C} \pi_k Beta(x_n \mid \alpha_k, \beta_k)} \quad (5)$$

In the M-step, the mixing proportion (π_c), and the parameters are updated given the expected value. The equation to update the mixing proportion is given by:

$$\pi_c^{i+1} = \frac{1}{N} \sum_{n=1}^{N} z_{nc} \quad (6)$$

The pair of parameters [α_c,β_c] are independent of any other pair for any value of c. These parameters should be updated simultaneously for each value of $c = 1, 2, ..., C$. First, the complete data log-likelihood function (3) is partially derived by α_c and β_c:

$$\frac{\partial L(\vartheta \mid X, Z)}{\partial \alpha_c} = \sum_{n}^{N} z_{nc}[logx_n + \psi(\alpha_c+\beta_c) - \psi(\alpha_c)] \quad (7)$$

$$\frac{\partial L(\vartheta \mid X, Z)}{\partial \beta_c} = \sum_{n}^{N} z_{nc}[log(1-x_n) + \psi(\alpha_c+\beta_c) - \psi(\beta_c)] \quad (8)$$

where $\psi(\cdot)$ is the digamma function defined by:

$$\psi(w) = \frac{\partial log\Gamma(w)}{\partial w} \quad (9)$$

To find a local maximum, both equations are equated to zero to form equation system.

$$\begin{bmatrix} \frac{\partial L(\vartheta|X,Z)}{\partial \alpha_c} \\ \\ \frac{\partial L(\vartheta|X,Z)}{\partial \beta_c} \end{bmatrix} = 0 \quad (10)$$

$$\begin{aligned} \psi(\alpha_c) - \psi(\alpha_c+\beta_c) &= \frac{\sum_n^N z_{nc} logx_n}{\sum_n^N z_{nc}} \\ \psi(\beta_c) - \psi(\alpha_c+\beta_c) &= \frac{\sum_n^N z_{nc} log(1-x_n)}{\sum_n^N z_{nc}} \end{aligned} \quad (11)$$

Since there is no closed solution to this equation system [27], the Newton-Raphson algorithm was used [31].

Parameter initialization

The EM algorithm is an iterative method which requires a parameter initialization to start. The result of this algorithm depends on this initialization. To obtain the initial values, a reference distribution was obtained [26]. This distribution is obtained by averaging 40 samples from the control group. The reference distribution is approximated by a BMM with four components. A fixed number of four components was chosen for the model based on the high pressure areas and the symmetric butterfly pattern (Fig. 4). The parameters obtained served as initial values to approximate the sample distributions of the control and DM group (Fig. 4 and Table 1). Chi-square goodness-of-fit was obtained to numerically measure how the BMM fits the distribution, resulting in 1.45×10^{-3}.

TABLE 1. Final parameters of the beta mixture model (BMM) approach for the reference distribution

	Component 1 (Toes)	Component 2 (Metatarsal heads)	Component 3 (Arch)	Component 4 (Heel)
α	1.89	8.35	5.24	5.59
β	7.86	24.05	3.66	1.59
π	0.17	0.05	0.33	0.45

This article has been accepted for publication in a future issue of this journal, but has not been fully edited. Content may change prior to final publication. Citation information: DOI 10.1109/ACCESS.2019.2902502, IEEE Access

TABLE 2. Parameter values of the Beta mixture model (BMM) components presented in Fig. 5

	Component 1 (Toes)			Component 2 (Metatarsal Heads)			Component 3 (Arch)			Component 4 (Heel)		
	α	β	π	α	β	π	α	β	π	α	β	π
Fig. 5a	1.42	3.60	0.13	11.20	8.30	0.170	3.61	8.25	0.18	2.91	1.54	0.52
Fig. 5b	1.62	3.35	0.09	15.44	11.19	0.18	5.44	11.68	0.15	3.19	1.54	0.57
Fig. 5c	1.77	5.96	0.16	13.03	11.74	0.16	2.67	5.40	0.17	3.94	2.00	0.52
Fig. 5d	2.01	10.88	0.22	7.16	6.561	0.11	3.38	7.05	0.20	3.30	1.43	0.47
Fig. 5e	1.80	8.13	0.21	10.23	10.26	0.12	3.73	7.25	0.20	3.96	1.54	0.47
Fig. 5f	2.27	9.13	0.23	3.41	11.68	0.33	3.41	3.33	0.06	4.09	1.47	0.38

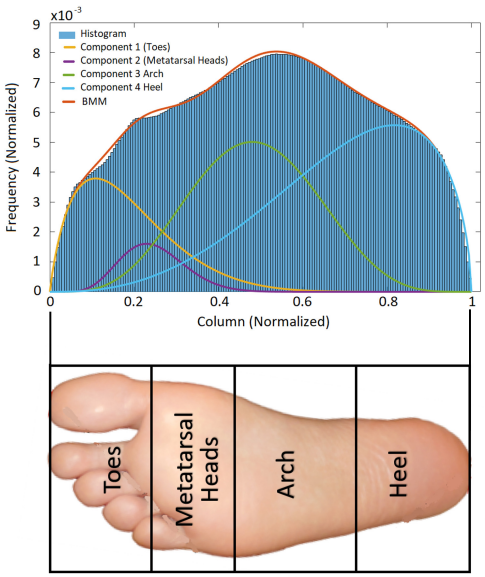

FIGURE 4. Approximation of the reference distribution by a Beta mixture model (BMM) with four components, each representing an area of the plantar region: toes, metatarsal heads, arch and heel.

3) Convergence

In this work, the convergence of the algorithm is determined by verifying the value between the log-likelihood function (3) in each iteration. The relative change is used as the convergence parameter instead of the absolute value of change in the log-likelihood function since it depends on the sample size. The threshold to detect the convergence in this work was $E = 0.0001$. and the maximum number of iterations was established in $I = 1000$.

III. EXPERIMENTAL RESULTS

For the tests, 111 thermograms of the DM group and 30 thermograms of the control group were used. The left and right foot were automatically segmented, and each was taken as a separate sample. In the DM group, two feet were excluded from the tests by infection or amputation, obtaining a database of 280 samples. Each sample was modeled using a BMM with four components representing four different areas in the plantar region. The EM algorithm was initialized with the parameters obtained from the reference distribution (Table 1) and ends when the relative change of the the log-likelihood function (3) in two consecutive iterations is below the established value ($E = 0.0001$).

Fig. 5 and Table 2 show examples of the approach by BMM with their respective values of α, β and π. Also, Chi-square goodness-of-fit was used to measure the accuracy of the model to fit the temperature distributions. For the control group, an average of $(3.49 \times 10^{-3}) \pm (1.94 \times 10^{-3})$ was obtained, and for the DM group, the average was $(6.18 \times 10^{-3}) \pm (2.23 \times 10^{-3})$.

The mean and the variance of each component of the BMM was calculated, and the results are presented in Table 3. The greatest variations were found in components 1 and 4 (toes and heel). Figure 6 shows the data set plotted by the mean of the component 1 and 4, respectively. The K-means algorithm was applied to automatically split the data set into different clusters (see Fig. 6). Some examples of the temperature distributions of each cluster are shown in Fig. 7. Based on these distributions, red points (cluster 1) represent the distributions without variation. Cluster 2 (blue points) contains the distributions with upper area variation, while cluster 3 (green points) includes distributions with variation in the whole foot.

TABLE 3. Average of the mean and variance of each component of the Beta mixture model (BMM) (average $\pm$ standard deviation)

	Control Group		DM Group	
	Mean	Variance	Mean	Variance
1	0.32 ± 0.10	0.04 ± 0.018	0.21 ± 0.10	0.02 ± 0.018
2	0.56 ± 0.03	0.01 ± 0.003	0.55 ± 0.06	0.01 ± 0.010
3	0.32 ± 0.02	0.02 ± 0.005	0.33 ± 0.04	0.01 ± 0.005
4	0.65 ± 0.03	0.04 ± 0.007	0.70 ± 0.07	0.03 ± 0.015

IV. DISCUSSION

Due to the variation in the α and β parameters, it was not possible to categorize the temperature distributions with these parameters. However, when the mean and variance were calculated, it was possible to properly separate the distributions. The greatest variation between groups is found in the mean of component 1 (toes), with an average of 0.32 ± 0.10 for the control group and 0.21 ± 0.10 for DM group (Table 3). This variation allows for the identification of the temperature distribution with variation in the upper area of the foot. The variation in component 4 (heel) also allows to identify distributions with variation in the lower part, with an average of 0.65 ± 0.03 for the control group

This article has been accepted for publication in a future issue of this journal, but has not been fully edited. Content may change prior to final publication. Citation information: DOI 10.1109/ACCESS.2019.2902502, IEEE Access

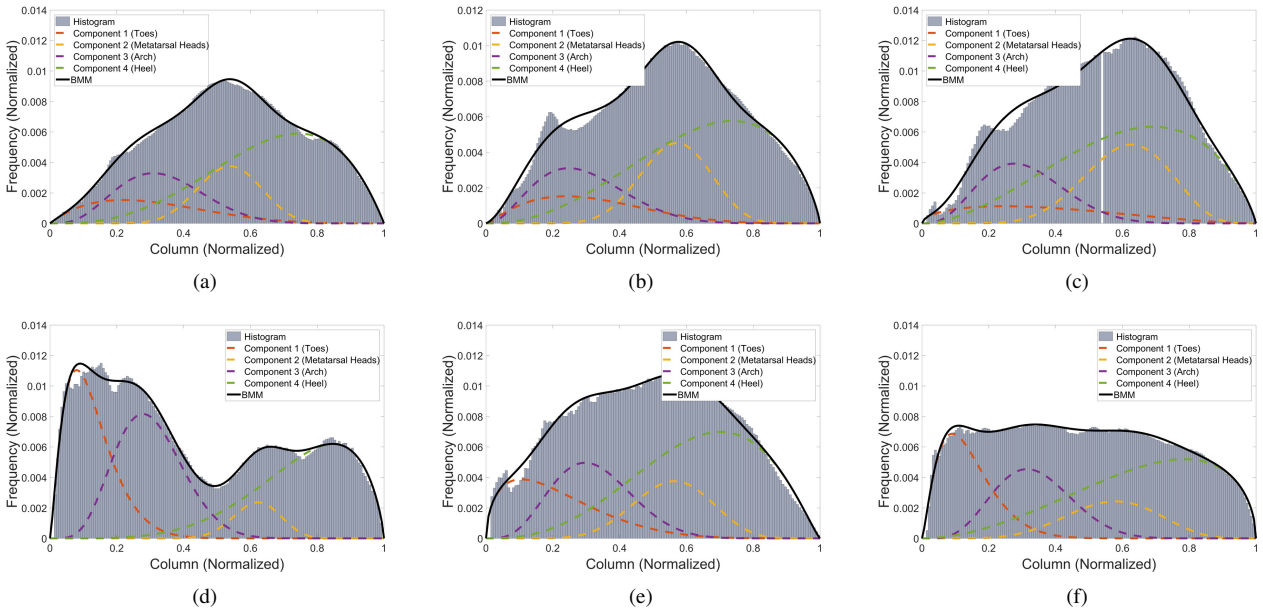

FIGURE 5. Examples of the approach by Beta mixture model (BMM) of the temperature distribution in (a-c), control group and (d-f) DM group. The Chi-square goodness-of-fit was calculated in each distribution: a) 1.70×10^{-3}, b) 4.64×10^{-3}, c) 8.74×10^{-3}, d) 6.40×10^{-3}, e) 6.30×10^{-3}, f) 4.10×10^{-3}.

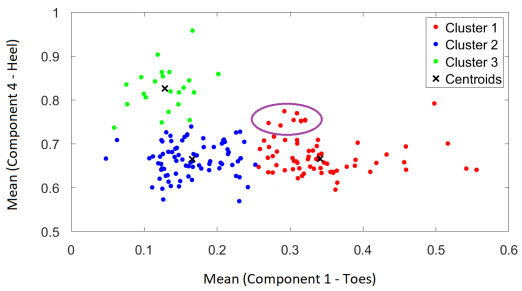

FIGURE 6. Data set plotted by the mean of the Beta components 1 and 4. K-means clustering is applied to split the data in 3 clusters.

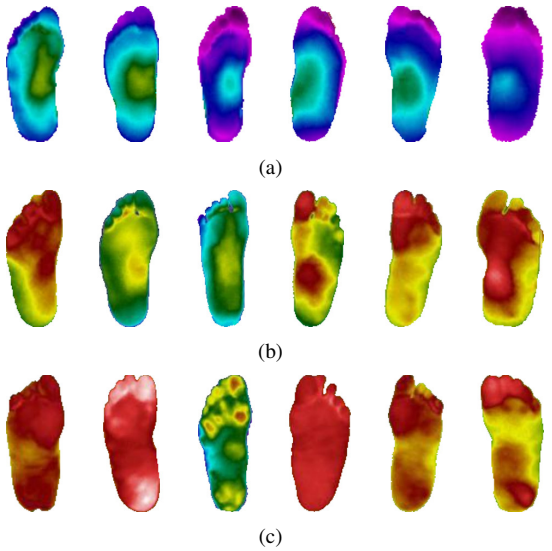

FIGURE 7. Examples of the temperature distributions of each cluster in Fig. 6. (a) Distributions without variations (Cluster 1); (b) distributions with upper area variations (Cluster 2) and (c) distributions with variations in the whole foot (Cluster 3).

in contrast to 0.70 ± 0.07 for DM group (Table 3). By using both characteristics, it was possible to identify the three previously mentioned groups. In cluster 1, temperature distributions with temperature changes only in the lower area (heel) were found (Fig. 8). These distributions (points enclosed in the purple oval in Fig. 6) have a mean value of component 1 in the range of cluster 1 (< 0.35), but these have the highest mean values of component 4 (> 0.75) in this cluster. However, these distributions were uncommon in our database, so the k-means algorithm included them in the closest cluster

To compare the performance of the BMM approach, the temperature distributions were fitted with different models. Figure 9 shows the comparison among BMMs with different number of components and initialized with the method of moments (MM). For MM initialization, first, the data is divided into k groups using the k-means algorithm, and after that, the moment estimators of the corresponding distribution are calculated.

The performance of the different approaches are compared with the chi-square goodness-of-fit (GoF) and the total of iterations, presented in Fig. 10 and Fig. 11 respectively. A smaller value in the GoF indicates a better fit. Of the distributions presented in the Fig. 10, the BMM proposed in this work presents a lower value than the other approximations in 7 of the 8 distributions. Also the number of iterations necessary for convergence is lower in 7 of the 8 distributions. Another aspect to consider is that with 4 components the

This article has been accepted for publication in a future issue of this journal, but has not been fully edited. Content may change prior to final publication. Citation information: DOI 10.1109/ACCESS.2019.2902502, IEEE Access

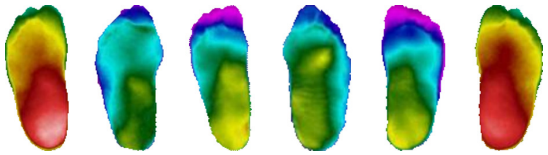

FIGURE 8. Temperature distributions with lower area variation found in cluster 1. Points enclosed in the purple oval in Fig. 6

.

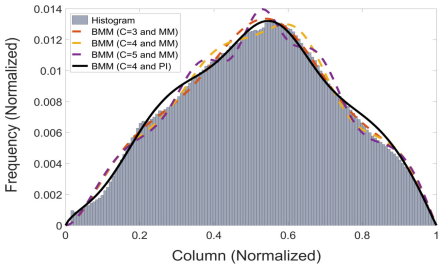

(a)

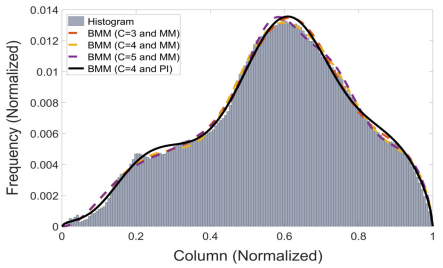

(b)

FIGURE 9. Comparison among Beta mixture models (BMMs), varying the number of components and initializing with the method of moments (MM)

analysis is simplified since each component is assigned to one of the areas (toes, metatarsal heads, arch and heel). For the database, the GoF average was 0.0064 ± 0.0013 for the proposed model while for the BMM with an MM initialization and a C value of 3, 4 and 5 the GoF was 0.0074 ± 0.0014, 0.0076 ± 0.0013 and 0.0081 ± 0.0021, respectively. This confirms a better performance of the BMM with $C = 4$ and initialized with the parameters of Table 1.

The model was also compared with a Gaussian mixture model (GMM) and Gamma mixture model (GmMM), both with different numbers of components (Fig. 12). Comparisons of the GoF and convergence iterations of the mixture models are presented in Figs. 13-16. In the GMM, the GoF presents a higher value in each of the distributions (Fig. 13), especially in the distributions of the DM group. As the number of components in the GMM increases, the GoF improves, however, the number of iterations also increases (Fig. 14). Therefore, to obtain a performance similar to the BMM, the number of components of the Gaussian model must be above 7. With a higher number of components, it is not possible to assign the components to a specific area, making the analysis more difficult.

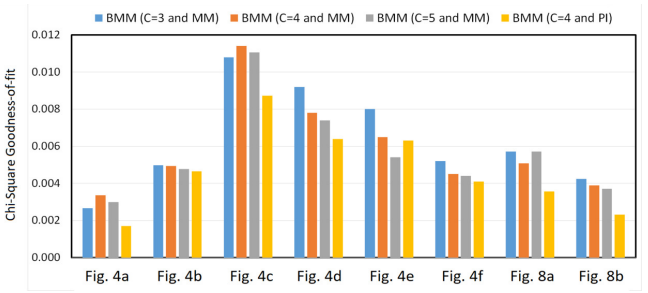

FIGURE 10. Comparison of the Chi-Square Goodness-of-fit for the distributions presented in Fig. 5 and Fig. 9. The yellow bar represents the proposed Beta mixture model (BMM), and this is compared with other BMM, varying the number of components and initialized with the method of moments (MM)

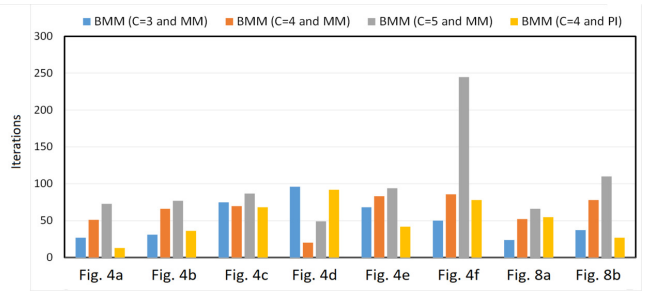

FIGURE 11. Comparison of the total iterations required for the convergence in the different Beta mixture models (BMMs)

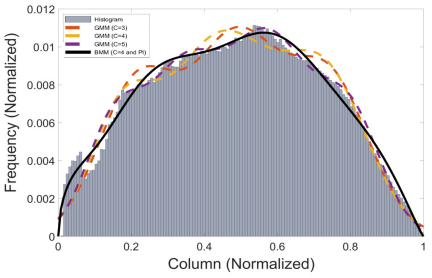

(a)

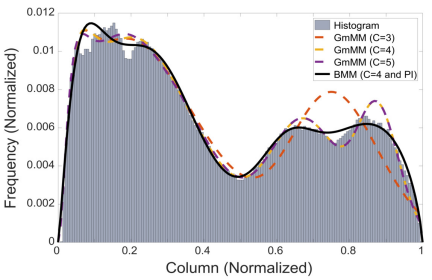

(b)

FIGURE 12. Comparison among Beta mixture models (BMM) with (a) Gaussian mixture model (GMM) and (c) Gamma mixture model (GmMM). Both approaches are tested with a different number of components and initializing with the method of moments (MM)

The GmMM presents better performance in several distributions than the GMM (Fig. 15), because it can be skewed to the left. For the GmMM, the lowest GoF average for

This article has been accepted for publication in a future issue of this journal, but has not been fully edited. Content may change prior to final publication. Citation information: DOI 10.1109/ACCESS.2019.2902502, IEEE Access

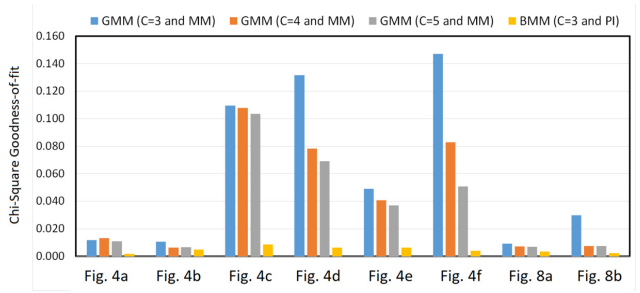

FIGURE 13. Comparison of the Chi-Square Goodness-of-fit for the distributions presented in Fig. 5 and Fig. 9. The yellow bar represents the proposed Beta mixture models (BMM), and this is compared with Gaussian mixture models (GMM), varying the number of components and initialized with the method of moments (MM)

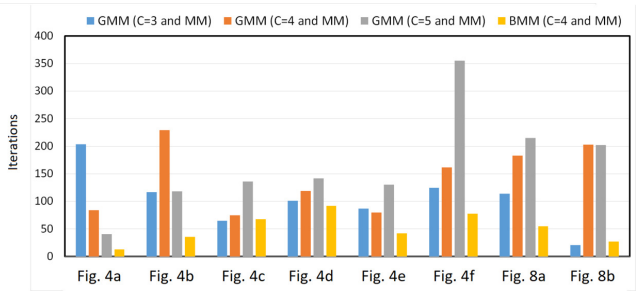

FIGURE 14. Comparison of the total iterations required for the convergence in the different Gaussian mixture model (GMM) and Beta mixture models (BMM)

all database was obtained with five components (0.0179 ± 0.0157), and this was lower than that obtained by the GMM (0.0264 ± 0.0351). Although the GmMM has a lower GoF average value than that presented by the GMM, the proposed BMM has a better performance (0.0064 ± 0.0013). The main problem occurs in those distributions where the asymmetry is to the right (Fig. 5c) resulting in high values in the GoF. Another problem is the high number of iterations required for convergence with an average of 879 ± 172 iterations and in several distributions the maximum number of iterations was not enough. (Fig. 16).

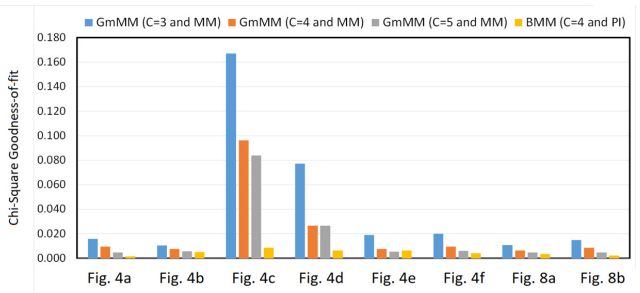

FIGURE 15. Comparison of the Chi-Square Goodness-of-fit for the distributions presented in Fig. 5 and Fig. 9. The yellow bar represents the proposed Beta mixture models (BMM), and this is compared with Gamma mixture models (GmMM), varying the number of components and initialized with the method of moments (MM)

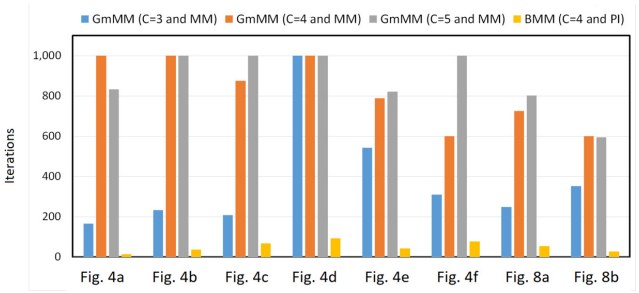

FIGURE 16. Comparison of the total iterations required for the convergence in the different Gamma mixture models (GmMM) and Beta mixture models (BMM)

V. CONCLUSION

A characterization of the plantar temperature distribution based on a BMM has been presented. The Beta components allow one to identify changes in the lower and upper area of the plantar region. The results showed that components 1 and 4, which represent the toes and the heel, show a greater variation between the control and the DM group. With these two components, it was possible to characterize changes in the plantar temperature distribution. The contributions of this approach is that it allows one to analyze thermal changes in different areas of the plantar region separately, and it is possible to detect temperature variations related to the diabetic foot, overcoming the limitations of asymmetric analysis. Each foot is analyzed separately, so the temperature variations can be detected even if the patients has a similar variation on both feet since it does not depend on a contralateral comparison.

VI. ACKNOWLEDGMENT

The author D. Hernandez-Contreras wants to thanks to the CONACYT for the financial support provided for his studies. The author also wants to thank Francisco Renero for his contributions to this work.

REFERENCES

[1] C. M. Clark Jr and D.A. Lee, "Prevention and treatment of the complications of diabetes mellitus," New Engl. J. Med., vol. 332, no. 18, pp. 1210-1217, 1995.

[2] C. D. Mathers Jr and D. Loncar, "Projections of global mortality and burden of disease from 2002 to 2030," PLOS Med., vol. 3, no. 11, pp. 442, 2006.

[3] J. Apelqvist and J. Larsson, "What is the most effective way to reduce incidence of amputation in the diabetic foot?," Diabetes Metab. Res., vol. 16, no. S1, pp. 75-83, 2000.

[4] N. C. Schaper et al., "Prevention and management of foot problems in diabetes: a Summary Guidance for Daily Practice 2015, based on the IWGDF Guidance Documents," Diabetes Metab. Res., vol. 32, pp. 7-15, 2016.

[5] A. Veves et al., "The risk of foot ulceration in diabetic patients with high foot pressure: a prospective study," Diabetologia, vol. 35, no. 7, pp. 660-663, 1992.

[6] R. G. Houdas and E.F.J. Ring, "Temperature distribution" in Human Body Temperature, Springer, 1982, pp. 81-103.

[7] R. G. Frykberg et al., "Diabetic foot disorders: a clinical practice guideline (2006 revision)," J. Foot Ankle Surg., vol. 45, no. 5, pp. S1-S66, 2006.

[8] F. J. Renero-C., "The thermoregulation of healthy individuals, overweight–obese, and diabetic from the plantar skin thermogram: a clue to predict the diabetic foot," Diabet. Foot Ankle, vol. 8, no. 1, p. 1361298, 2017.

[9] N. Zaproudina et al., "Plantar infrared thermography measurements and low back pain intensity," J. Manipulative Physiol. Ther., vol. 29, no. 3, pp. 219-223, 2006.
[10] J. Oliveira et al., "Use of infrared thermography for the diagnosis and grading of sprained ankle injuries," Infrared Phys. Techno., vol. 76, pp. 530-541, 2016.
[11] EY-K. Ng, 'A review of thermography as promising non-invasive detection modality for breast tumor," Int. J. Therm. Sci., vol. 48, no. 5, pp. 849-859, 2009.
[12] J. H. Tan et al., "Infrared thermography on ocular surface temperature: a review," Infrared Phys. Techno., vol. 52, no. 4, pp. 97-108, 2009.
[13] D. Hernandez-Contreras et al., "Automatic classification of thermal patterns in diabetic foot based on morphological pattern spectrum," Infrared Phys. Techno., vol. 73, pp. 149-157, 2015.
[14] N. Kaabouch et al., "Alternative technique to asymmetry analysis-based overlapping for foot ulcer examination: scalable scanning," J. Diabetes Metab., vol. 2012, 2012.
[15] T. Nagase et al., "Variations of plantar thermographic patterns in normal controls and non-ulcer diabetic patients: novel classification using angiosome concept," J. Plast. Reconstr. Aesthet. Surg., vol. 64, no. 7, pp. 860-866, 2011.
[16] T. Mori et al., "Morphological pattern classification system for plantar thermography of patients with diabetes," J. Diabetes Sci. Technol., 2013.
[17] C. Liu et al., "Automatic detection of diabetic foot complications with infrared thermography by asymmetric analysis," J. Biomed. Opt., vol. 20, no. 2, p. 026003, 2015.
[18] L. Vilcahuaman et al. (2015, June). Automatic Analysis of Plantar Foot Thermal Images in at-Risk Type II Diabetes by Using an Infrared Camera presented at IFMBE Proc. Available: https://link.springer.com/chapter/10.1007/978-3-319-19387-8_55
[19] H. Peregrina-Barreto et al., "Quantitative estimation of temperature variations in plantar angiosomes: a study case for diabetic foot," Comput. Math. Methods Med., vol. 2014, 2014.
[20] D. Hernandez-Contreras et al., "Narrative review: Diabetic foot and infrared thermography," Infrared Phys. Techno., vol. 78, pp. 105-117, 2016.
[21] M. Adam et al., "Computer aided diagnosis of diabetic foot using infrared thermography: A review," Comput. Biol. Med., vol. 91, pp. 326-336, 2017.
[22] A. W. Chan et al., "Contact thermography of painful diabetic neuropathic foot," Diabetes Care, vol. 14, no. 10, pp. 918-922, 1991.
[23] P.D. McNicholas, "Parameter Estimation" in Mixture Model-Based Classification, CRC Press, 2016.
[24] M. Bouguessa (2011). An unsupervised approach for identifying spammers in social networks presented at Proc. Int. C. Tools Art. Available: https://ieeexplore.ieee.org/abstract/document/6103421
[25] "Thermography guidelines: standards and protocols in clinical thermographic imaging" by International Academy of Clinical Thermology., IACT, 2002.
[26] D. Hernandez-Contreras et al. (2017). Measuring changes in the plantar temperature distribution in diabetic patients presented at IEEE IMTC P. Available: https://ieeexplore.ieee.org/abstract/document/7969699
[27] Z. Ma and A. Leijon (2009). Beta mixture models and the application to image classification presented at IEEE Image Proc. Available: https://ieeexplore.ieee.org/abstract/document/5414043
[28] C. Schröder and S. Rahmann, "A hybrid parameter estimation algorithm for beta mixtures and applications to methylation state classification," Algorithms Mol. Bio., vol. 12, no. 1, pp. 21, 2017.
[29] C.M. Bishop, "Pattern Recognition and Machine Learning", Information Science and Statistics, Springer, 2006.
[30] G. McLachlan and T. Krishnan, 'The EM Algorithm and Extensions", Wiley Series in Probability and Statistics, Wiley, 2007.
[31] C. T. Kelley, 'Solving nonlinear equations with Newton's method", Siam, 2003.

DANIEL ALEJANDRO HERNANDEZ CONTRERAS was born in Puebla, Mexico. He received the B.Sc. degree in mechatronic engineering from Popular Autonomous University of Puebla State (UPAEP), Mexico, and the M.Sc. degree in electronics from the National Institute of Astrophysics, Optics, and Electronics (INAOE), Mexico. He is currently studying for the Ph. D. degree in electronics with interest in the research of image and signal processing.

HAYDE PEREGRINA-BARRETO received her B.Sc. in computer engineering from Instituto Tecnologico de Cuautla, Mexico (2006), her M.Sc. in Engineering from Universidad de Guanajuato, Mexico (2008), and her Ph.D. in Engineering from the Universidad Autonoma de Queretaro, Mexico (2011). She is currently a full researcher at the Computer Science Department at INAOE, Mexico and member of the Mexican National Research System (SNI) level 1. Her research interests include medical image analysis and computer vision

JOSE DE JESUS RANGEL-MAGDALENO received the B.E. degree in electronics engineering and the M.E. degree in electrical engineering on hardware signal processing from Universidad de Guanajuato, Mexico in 2006 and 2008, respectively. He received the Ph.D. degree from the Universidad Autonoma de Queretaro, Mexico in 2011. He is currently Full Researcher at the Electronics Department at INAOE, Mexico. He has authored 1 book, and more than 75 works published in book chapters, journals and conferences. He is a member of the Mexican national research system (SNI), level 1. His research interests include FPGAs, signal and image processing, instrumentation and mechatronics.

FELIPE ORIHUELA-ESPINA received the Ph.D. degree from the University of Birmingham, Birmingham, U.K. He has been a Lecturer at Universidad Autonoma del Estado de MÃl'xico and a Postdoctoral Research Associate at Imperial College London from 2007 to 2010 and at the National Institute for Astrophysics, Optics and Electronics (INAOE), Puebla, Mexico, from 2010 to 2012. He is currently a Senior Lecturer at INAOE and member of the Mexican National Research System (SNI-1). He has authored over 80 peer-reviewed full-length articles and book chapters including 38 JCR indexed journal papers. His current research interests are in fNIRS neuroimaging understanding and interpretation.